A TWO-DIMENSIONAL GLOBAL DISPERSION MODEL APPLIED TO SEVERAL HALOCARBONS

by

DEBRA KAY WEISENSTEIN

S.B., Massachusetts Institute of Technology
(1978)

S.B., Massachusetts Institute of Technology
(1978)

SUBMITTED TO THE DEPARTMENT OF
METOEROLOGY AND PHYSICAL OCEANOGRAPHY
IN PARTIAL FULFILLMENT OF THE
REQUIREMENTS FOR THE DEGREE OF

MASTER OF SCIENCE

at the

MASSACHUSETTS INSTITUTE OF TECHNOLOGY

January 1983

Signature of Author _____
Dept. of Meteorology and Physical Oceanography

Certified by _____
Thesis Supervisor

Accepted by _____
Chairman, Department Committee

Abstract

This thesis investigates the use of a Lagrangian mean wind field in a two-dimensional tracer transport model. Advection by the Lagrangian mean circulation accounts for approximately 90% of the horizontal transport and all of the vertical transport in the model. A horizontal diffusion coefficient of 1.0×10^{10} cm^2/sec was introduced into the model to account for the variance in wind velocities, since the model uses seasonally-averaged wind fields.

The model was applied to three chemical species: carbon tetrachloride, trichlorofluoromethane, and dichlorodifluoromethane. These halocarbons are of interest because of their potential for catalytic destruction of ozone in the stratosphere. They are primarily of anthropogenic origin and are modeled as having a source at ground level and a sink due to photodissociation in the stratosphere. The photodissociation lifetimes and the global and ground level trends were calculated and compared to observations obtained by the Atmospheric Lifetime Experiment.

Table of Contents

List of Tables

List of Figures

I. Introduction

Two-dimensional models of tracer transport have traditionally employed advection by the zonally averaged mean meridional circulation and gradient-induced flow parameterized in terms of eddy diffusion.

Tracer experiments have shown that the atmospheric mean mass flow, especially in the stratosphere, does not look like the Eulerian mean meridional circulation but more closely resembles the "Brewer-Dobson" circulation. (See Dutsch, 1971.) The explanation is that the eddy fluxes are just as important as the mean meridional circulation in determining the magnitude and direction of mass transport in the atmosphere. In fact, the Eulerian mean transport and the eddy transport almost cancel. Thus the net zonally averaged transport is the small residual obtained by summing two large terms of opposite sign. This approach is subject to numerical error and the empirical determination of diffusion coefficients lacks a physical basis.

Dunkerton (1978) treated the transport problem as purely advective by the use of a Lagrangian mean circulation. He calculated a set of Lagrangian mean wind velocities using the thermodynamic and continuity equations and simplifying under the assumption that meridional temperature advection and vertical eddy fluxes were small. Dunkerton arrived at a simplified balance equation relating diabatic heating and static stability to the Lagrangian mean wind velocities. He was able to show that this circulation resembled the "Brewer-Dobson" circulation.

Olaguer (1982) followed the approach of Dunkerton but did not neglect meridional temperature advection or wave dissipation. He calculated a Lagrangian mean circulation for the solstices based on mutually-consistent temperature and diabatic heating profiles from a run of the MIT three-dimensional stratospheric model. His Lagrangian mean velocities, with some smoothing, are used in our two-dimensional tracer transport model.

Holton (1981) used the theory of the residual mean meridional circulation

to develop an Eulerian two-dimensional advective model of stratospheric tracer transport. The residual mean meridional circulation, as defined by Andrews and McIntyre (1976), is the difference between the Eulerian mean circulation and the eddy-induced circulation. This definition removes all eddy terms from the thermodynamic and transport equations if the eddy field is steady and adiabatic. The residual mean circulation used by Holton was calculated from the output of the Holton and Wehrbein three-dimensional model and included the effects of diabatic heating, wave transience, and dissipation. Holton applied his residual mean circulation to the transport of N_2O and found qualitative agreement with observed tracer profiles.

Tung (1982) approached the problem of the residual mean circulation with the use of isentropic coordinates. He showed that the zonal mean circulation calculated in isentropic coordinates is the mean diabatic circulation. This circulation is thermally direct and is in the same direction as tracer transport trajectories. Tung used Eulerian coordinates in his formulation to retain applicability to conventionally-obtained atmospheric data. However, he also showed that advective velocities in isentropic coordinates are approximately the Lagrangian mean velocities for the case of steady, conservative eddy fields and inert tracers.

Our model is an attempt to calculate the transport of tracers due to advection by the Lagrangian mean circulation, as formulated by Dunkerton and Olaguer. With tracer transport occurring by advection only, large concentration gradients were produced in our tracer concentration fields by allowing the same velocity field to operate on the tracer for a full season. The real atmosphere does not possess such strong concentration gradients because of mixing due to eddies and a large variance about the mean wind. We therefore introduced a diffusion term into the transport equation which smooths the concentrations and keeps concentration gradients within reasonable limits. The largely advective nature of our model is demonstrated by

separately monitoring the amount of transport due to advection and the amount due to diffusion. Diffusion accounted for an average of 15% of the horizontal transport crossing the equator and an average of 8.5% of the total horizontal transport. All vertical transport was due to advection.

II. The Model

1. The differential equations

The model used in this thesis was derived from the two-dimensional model of Pitari and Visconti (1980). However, it differs from their model in that it uses Lagrangian velocities, has only horizontal diffusion, and includes industrial input to the lower boundary. It also has a revised scheme for evaluating the transport term and different boundary conditions.

The differential equation to be solved by the model and integrated in a forward time-stepping scheme is:

$$\frac{\partial Q}{\partial t} = \left(\frac{\partial Q}{\partial t}\right)^{ind} + \left(\frac{\partial Q}{\partial t}\right)^{trans} + \left(\frac{\partial Q}{\partial t}\right)^{chem}$$

where Q=molecular number density of tracer,

X=number mixing ratio of tracer=Q/ρ,

ρ=molecular number density of air,

$(\partial Q/\partial t)^{ind}$=industrial input of tracer to atmosphere,

$(\partial Q/\partial t)^{trans}$=net molecular transport of tracer,

$(\partial Q/\partial t)^{chem}$=net chemical production or destruction of tracer.

In spherical coordinates, the transport term can be written as:

$$\left(\frac{\partial Q}{\partial t}\right)^{trans} = \frac{1}{\cos\phi}\left[-\frac{\partial}{a\partial\phi}(v\rho\cos\phi X) - \frac{\partial}{\partial z}(w\rho\cos\phi X) + \frac{\partial}{a\partial\phi}\left(K_{yy}\rho\cos\phi\frac{\partial X}{a\partial\phi}\right)\right]$$

where ϕ,z are coordinates in the latitudinal and vertical directions, v,w are Lagrangian mean velocities in the northward and upward directions, and a is the radius of the earth.

The chemistry term includes only photodissociation by ultraviolet radiation. It can be expressed in terms of a rate constant J.

$$\left(\frac{\partial Q}{\partial t}\right)^{chem} = -QJ.$$

2. The grid

The differential equation is solved in finite difference form on a grid from 80.5°N to 80.5°S and from the ground to an elevation of 71.6 km. Grid

points are spaced every 11.5 degrees of latitude and every 2.864 km in the vertical. The grid spacing was chosen to duplicate that used in the derivation of the Lagrangian mean wind velocities.

The grid point levels are numbered from 1 to 26, with level 1 at 71.6 km and level 26 at the ground. The 15 latitudes are numbered from north to south, beginning at 80.5°N. Grid point (i,j) will be used in this paper to represent the grid point at latitude i and level j.

3. The finite difference equations

In finite difference form, $\Delta Q/\Delta t$ is the sum of three finite difference terms.

$$\left(\frac{\Delta Q}{\Delta t}\right)_{i,j} = \left(\frac{\Delta Q}{\Delta t}\right)^{ind}_{i,j} + \left(\frac{\Delta Q}{\Delta t}\right)^{trans}_{i,j} + \left(\frac{\Delta Q}{\Delta t}\right)^{chem}_{i,j}$$

a) Industrial source term

The industrial source term represents the release to the atmosphere of a pollutant of industrial or domestic origin. Since such sources are at or near ground level, this term is applied only to the lowest two layers of grid points, implying that the tracer is well mixed up to 4.3 km above the ground within a few model time steps. The total annual anthropogenic release of the tracer and the latitudinal distribution of its release are input to the model. The model then calculates the number of molecules of tracer per square centimeter to be added to the ground level grid points at each time step such that the same mixing ratio is added to the two lowest grid points at each latitude.

b) Transport term

The transport term represents the movement of tracer between grid points within the model. Mass conservation is ensured by enforcing continuity on the assumed Lagrangian mean velocity field. The velocities obey the continuity equation as written here in spherical coordinates:

$$\frac{\partial}{a\partial\phi}(v\rho\cos\phi) + \frac{\partial}{\partial z}(w\rho\cos\phi) = 0$$

To minimize numerical instability, the finite differences were taken across a distance of one grid space, i.e. the difference was taken from half a grid space on one side of a point to half a grid space on the other side of the point. Mixing ratios midway between grid points were equated with the linear average of the mixing ratios of the two nearest points.

$$X_{i+1/2,j} = 0.5(X_{i,j} + X_{i+1,j})$$

$$X_{i,j+1/2} = 0.5(X_{i,j} + X_{i,j+1})$$

Velocities midway between grid points were found by averaging the mass flux between adjacent grid points.

$$(v\rho\cos\phi)_{i+1/2,j} = 0.5[(v\rho\cos\phi)_{i,j} + (v\rho\cos\phi)_{i+1,j}]$$

$$(w\rho\cos\phi)_{i,j+1/2} = 0.5[(w\rho\cos\phi)_{i,j} + (w\rho\cos\phi)_{i,j+1}]$$

It can be shown that the field of velocities at the points midway between grid points also satisfies continuity. Note that our modified velocity field has the horizontal and vertical velocities defined at different points. See Figure 1 for an illustration.

The finite difference equation for the transport term becomes:

$$\left(\frac{\Delta Q}{\Delta t}\right)^{trans}_{i,j} = \frac{1}{\cos\phi_i}\left\{\left[\left(\frac{-v\rho\cos\phi}{a\Delta\phi}\right)_{i-1/2,j} X_{i-1/2,j} - \left(\frac{-v\rho\cos\phi}{a\Delta\phi}\right)_{i+1/2,j} X_{i+1/2,j}\right]\right.$$

$$+ \left[\left(\frac{-w\rho\cos\phi}{\Delta z}\right)_{i,j-1/2} X_{i,j-1/2} - \left(\frac{-w\rho\cos\phi}{\Delta z}\right)_{i,j+1/2} X_{i,j+1/2}\right]$$

$$\left. + \left[\left(\frac{K_{yy}\rho\cos\phi}{(a\Delta\phi)^2}\right)_{i-1/2,j} (X_{i-1,j} - X_{i,j}) - \left(\frac{K_{yy}\rho\cos\phi}{(a\Delta\phi)^2}\right)_{i+1/2,j} (X_{i,j} - X_{i+1,j})\right]\right\}.$$

The horizontal dispersion coefficient K_{yy} is a parameterization meant to account for atmospheric eddies which disperse the tracer more uniformly than seasonally averaged Lagrangian transport could.

c) Chemistry term

The change in the tracer concentration at a grid point due to photodissociation is proportional to the concentration at that grid point and to the photodissociation coefficient, J.

$$\left(\frac{\Delta Q}{\Delta t}\right)^{chem}_{i,j} = -Q_{i,j} J_{i,j}$$

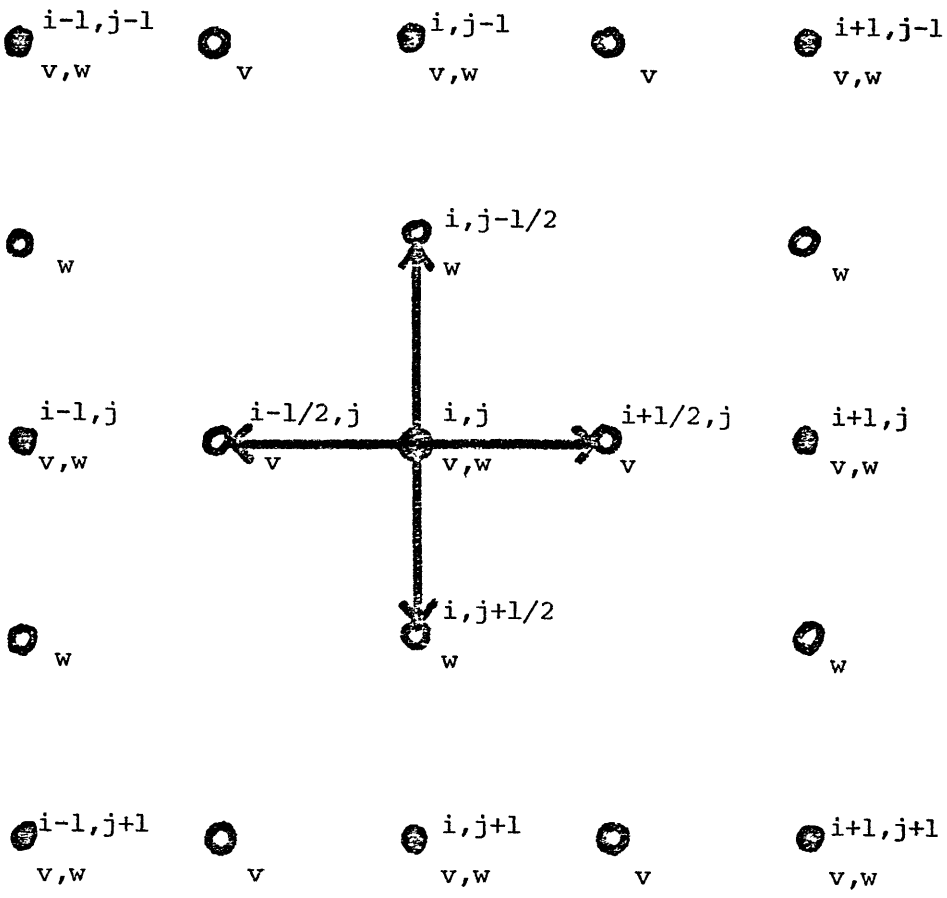

Figure 1: Sample of model grid. Solid dots represent model grid points at which tracer concentration is predicted and for which v and w are defined. Arrows show distance across which vertical and horizontal differences are taken and for which only v or w is defined.

4. Boundary Conditions

The boundary conditions are that no mass crosses the boundaries of the model. This constraint is applied by setting the horizontal Lagrangian wind velocities at 80.5°N and 80.5°S to zero, setting the vertical Lagrangian wind velocities at level 1 and level 26 to zero, and setting $\partial X/\partial y$ to zero at the side boundaries. Finite differences at the boundaries are uncentered and are taken over half of the normal distance.

At the left side boundary, 80.5°N, the transport term becomes:

$$\left(\frac{\Delta Q}{\Delta t}\right)^{trans}_{1,j} = \frac{1}{\cos\phi_1}\left\{ -\left(\frac{-v\rho\cos\phi}{0.5a\Delta\phi}\right)_{1+1/2,j} X_{1+1/2,j} + \left[\left(\frac{-w\rho\cos\phi}{\Delta z}\right)_{1,j-1/2} X_{1,j-1/2} - \left(\frac{-w\rho\cos\phi}{\Delta z}\right)_{1,j+1/2} X_{1,j+1/2}\right] + -\left(\frac{K_{yy}\rho\cos\phi}{0.5(a\Delta\phi)^2}\right)_{1+1/2,j}(X_{1,j}-X_{2,j})\right\}.$$

and similarly for the right side boundary. At the lower boundary, the transport term is:

$$\left(\frac{\Delta Q}{\Delta t}\right)^{trans}_{i,26} = \frac{1}{\cos\phi_i}\left\{\left[\left(\frac{-v\rho\cos\phi}{a\Delta\phi}\right)_{i-1/2,26} X_{i-1/2,26} - \left(\frac{-v\rho\cos\phi}{a\Delta\phi}\right)_{i+1/2,26} X_{i+1/2,26}\right] + \left(\frac{-w\rho\cos\phi}{0.5\Delta z}\right)_{i,26-1/2} X_{i,26-1/2} + \left[\left(\frac{K_{yy}\rho\cos\phi}{(a\Delta\phi)^2}\right)_{i-1/2,26}(X_{i-1,26}-X_{i,26}) - \left(\frac{K_{yy}\rho\cos\phi}{(a\Delta\phi)^2}\right)_{i+1/2,26}(X_{i,26}-X_{i+1,26})\right]\right\}.$$

5. Integration

Time integration of the finite difference equation is performed with the Lorenz 4-cycle time differencing scheme (Lorenz, 1971). The sum of the transport and chemistry terms is multiplied by a constant times the time step interval in seconds and added to the concentration at each grid point. The time step is 6 hours, and the 4-cycle scheme is complete, yielding second order time integration precision, every 24 hours.

The value of Q after the Nth cycle, using a time step of Δt, is:

$$Q(t+\Delta t)_{i,j} = Q(t)_{i,j} + Z(t)_{i,j}.$$

For N=1, $\quad Z(t)_{i,j} = \Delta t(\Delta Q/\Delta t)_{i,j}$,

$$N=2,3,4,\quad Z(t)_{i,j} = -(N-1)/(5-N)\ Z(t-\Delta t)_{i,j} + 4\Delta t/(5-N)(\Delta Q/\Delta t)_{i,j},$$

$$\text{where } \left(\frac{\Delta Q}{\Delta t}\right)_{i,j} = \left(\frac{\Delta Q}{\Delta t}\right)^{trans}_{i,j} + \left(\frac{\Delta Q}{\Delta t}\right)^{chem}_{i,j}.$$

The industrial source term, in molecules per cubic centimeter per day, is added to Q after a cycle of four time steps is completed.

$$Q(t+\Delta t)_{i,j} = Q(t)_{i,j} + 4\Delta t\left(\frac{\Delta Q}{\Delta t}\right)^{ind}_{i,j}$$

When an integration resulted in the concentration at a grid point being less than zero, it was set to zero and the necessary tracer mass was "borrowed" from neighboring grid points so as to avoid having unaccounted losses of mass from the system. Our technique was similar to that of Mahlman and Moxim (1978) except that tracer mass was borrowed equally from all suitable neighboring grid points. Suitable neighboring grid points had tracer concentrations at least as great as the magnitude of the negative grid point concentration. Negative concentrations were produced mainly above 30 km and the mass transport associated with "borrowing" to fill them in was at least 8 orders of magnitude less than the model transport due to advection.

6. Data

Our two-dimensional model uses seasonally averaged data. Temperatures, photodissociation coefficients, Lagrangian mean wind velocities, and horizontal diffusion coefficients are input for each season. The Northern Hemisphere winter season is December, January, and February.

The temperature values are those used by Pitari and Visconti (1980) and are derived from Dopplick (1972) below 30 km and Run 17 of the MIT three-dimensional model above 30 km. The photodissociation coefficients are calculated seasonally from cross-sections for the appropriate chemical species by a separate program which accounts for Rayleigh scattering in the calculation, as described by Pitari and Visconti (1978).

The Lagrangian mean velocity fields were derived from those calculated by E. Olaguer (1982). He calculated v and w for each day of January and July using daily values of density, potential temperature, and heating rate derived from runs of the MIT three-dimensional model. Daily values of v and w were averaged to give January and July monthly average velocities. Olaguer's calculation of Lagrangian mean velocities is described in Appendix A.

Because Olaguer's Lagrangian mean velocity field was derived from two months of data from one run of a specific model, his velocity fields were not as smooth as we desired for the climatological application needed in our model. For this reason, we found it necessary to smooth the velocity fields. Starting with the monthly averaged Lagrangian wind velocities, we applied continuity to produce a w field derived from the v field so that continuity was satisfied with our density fields. Deviations from Olaguer's w field were small. All values of w greater than 8 km/day were treated as missing and replaced by interpolation, since these values appeared to be unrealistic for our application. Six of the 390 January values and 10 of the 390 July values of w were replaced. A triangular smoothing function was then applied to the w momentum field ($w\rho\cos\phi$). Smoothing included two points to either side of a given point in the vertical and one point to either side in the horizontal. We applied continuity twice more, going from w to v and then from v to w, yielding velocity fields which satisfied continuity and which had v=0 at the side boundaries and w=0 at the top and bottom boundaries.

Seasonal values of Lagrangian velocities were obtained by assuming that the wind speeds vary sinusoidally with the seasons. The following time variation equation was applied and averaged over the seasons:

$$v(x,z,t)=0.5(v_S+v_W) + 0.5(v_S-v_W)\cos(2\pi t/360)$$

where v_S and v_W are the July and January average meridional velocities and t

is the number of days past July 15. A similar equation applies to the average vertical velocities.

For seasonal averages that represent a climatological mean, we wanted the Northern Hemisphere winter circulation to be similar to the Southern Hemisphere winter circulation six months later. To achieve this, we averaged the velocities for each season over both hemispheres and again checked continuity. See Figures 2-5 for the seasonally averaged Lagrangian velocity fields for winter-summer and spring-fall that were used in our model.

With only advective transport, our concentration fields frequently showed increasing tracer concentrations from the ground up to 20 km. With the K_{yy} field set at 1.0×10^{10} cm^2/sec for all latitudes, heights, and seasons, maximum concentrations appeared at or near ground level. The concentration field was adequately smooth and the largely advective character of the model was maintained. Other K_{yy} values tried were 1.0×10^9 and 5.0×10^9, but they were found to produce inadequate smoothing. Vertical diffusion coefficients of 1.0×10^5 in the troposphere and 1.0×10^2 in the stratosphere were also tried, but they were found to be unnecessary and, in addition, to produce too much upward transport of tracer as compared to observations.

7. Model constraints

The time step used in the model is constrained to be less than that which would cause mass to be advected across a distance of one grid space. In our case, the maximum horizontal and vertical velocities are 2471 cm/sec and 4.197 cm/sec, respectively. The grid spacing is 1278 km in the horizontal and 2.864 km in the vertical. This implies that our time step must be less than 14 hours. Our 6 hour time step satisfies this constraint.

Our model does not account for possible sources and sinks of tracer except for anthropogenic release at ground level and photodissociation in the stratosphere. Other possible sources include an oceanic flux, chemical reactions in the atmosphere, or other natural sources. The oceans and the

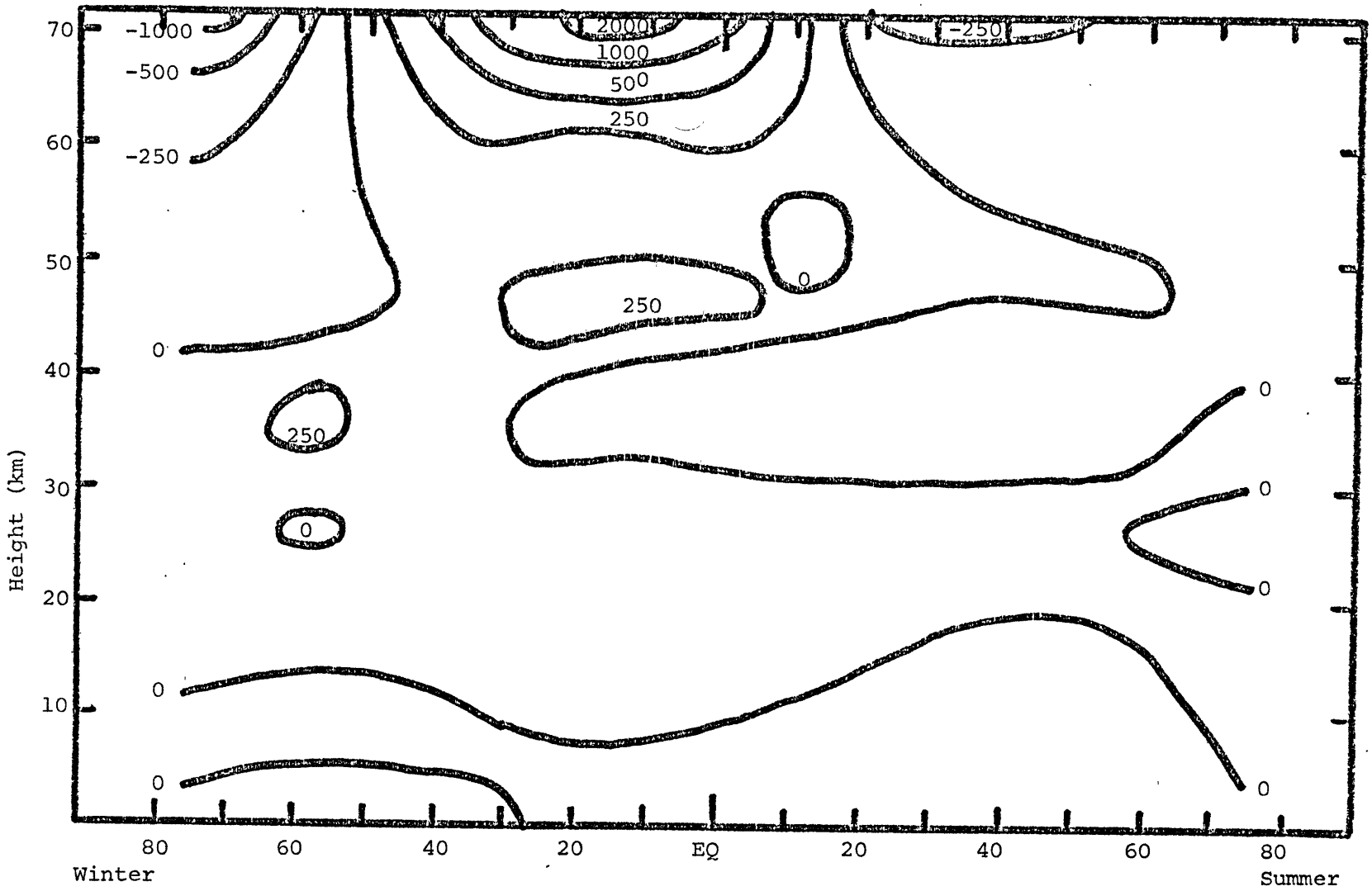

Figure 2: Lagrangian mean meridional wind velocities in cm/sec for winter and summer.

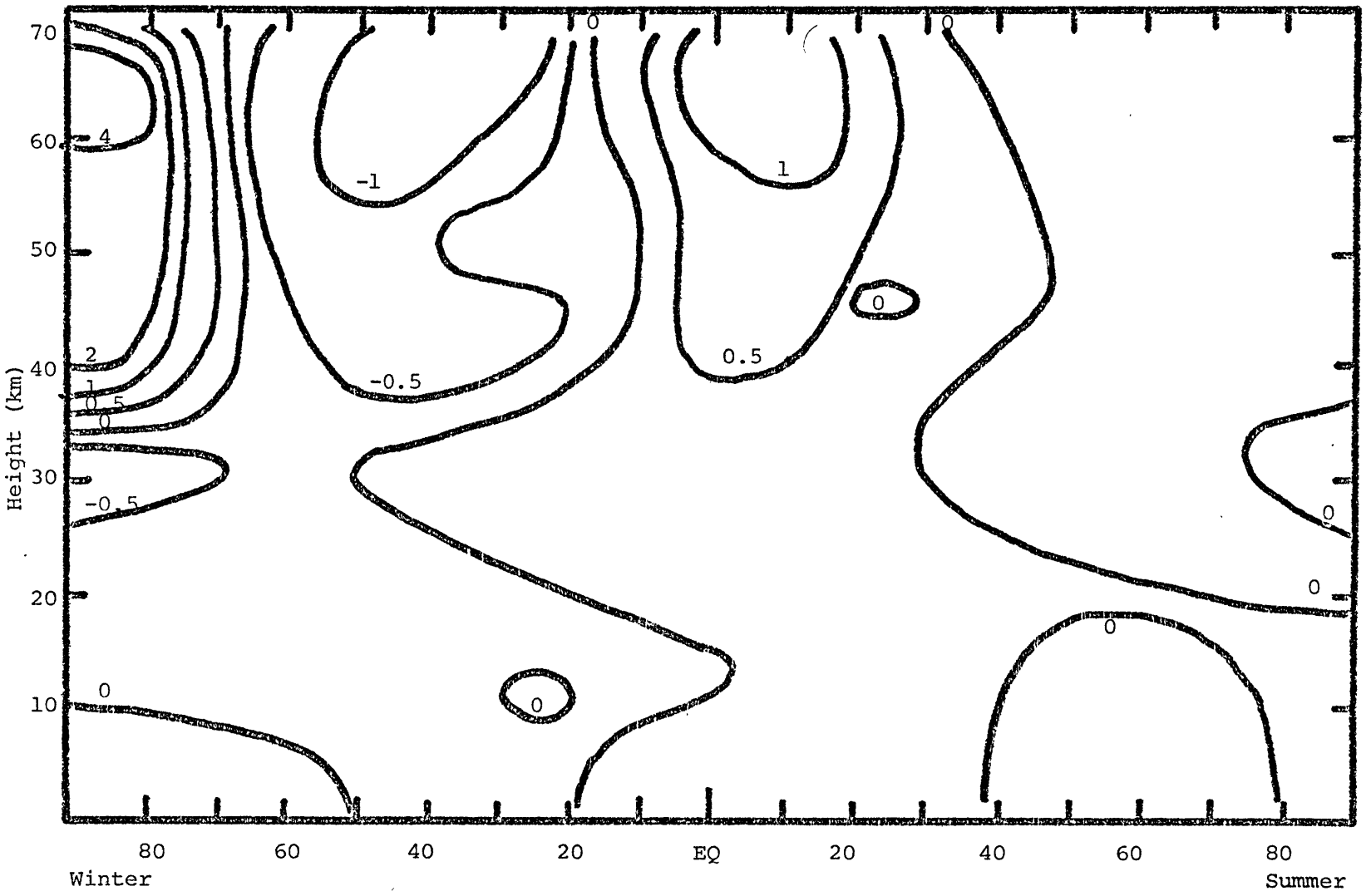

Figure 3: Lagrangian mean vertical wind velocities in cm/sec for winter and summer.

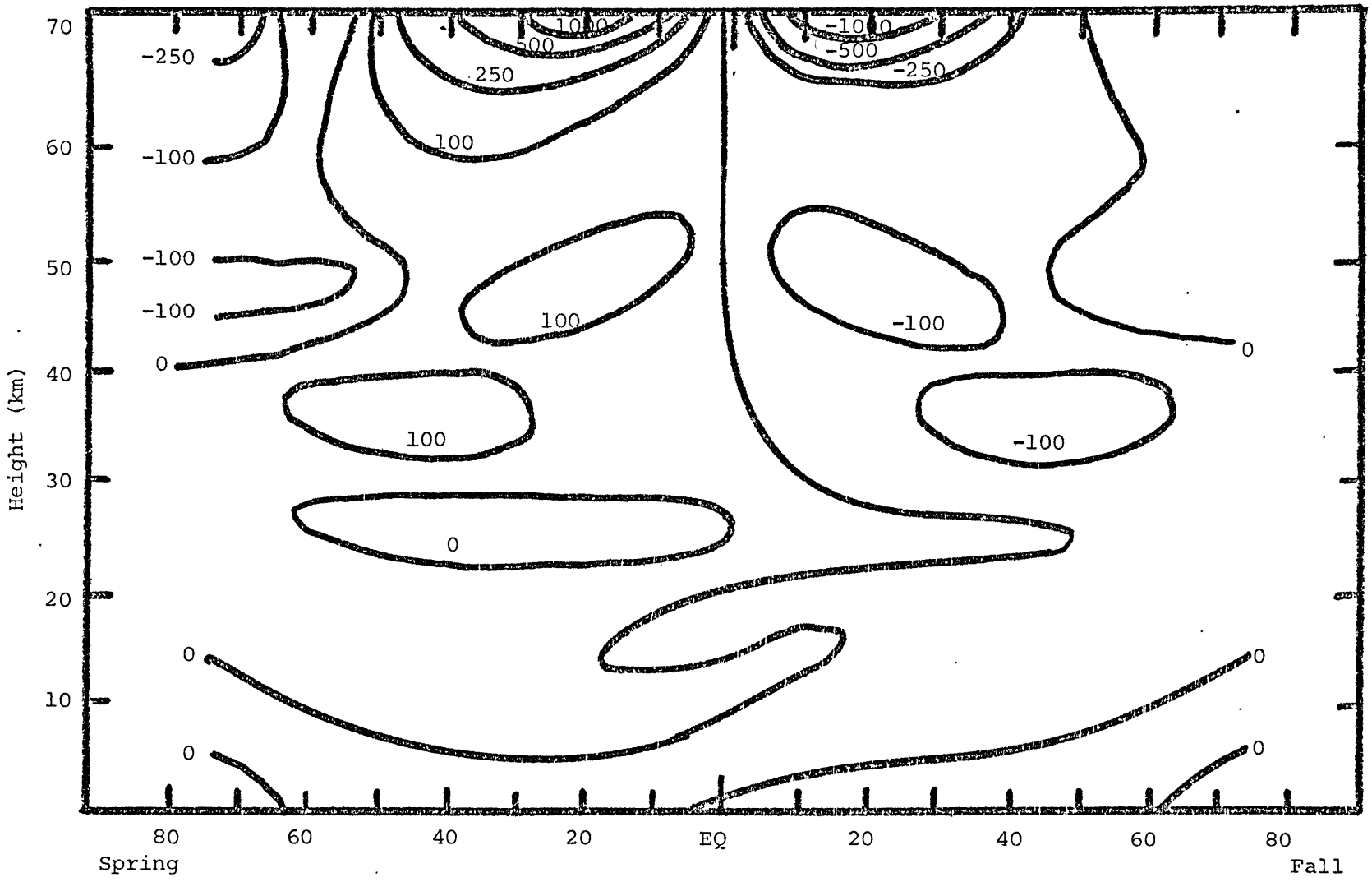

Figure 4: Lagrangian mean meridional wind velocities in cm/sec for spring and fall.

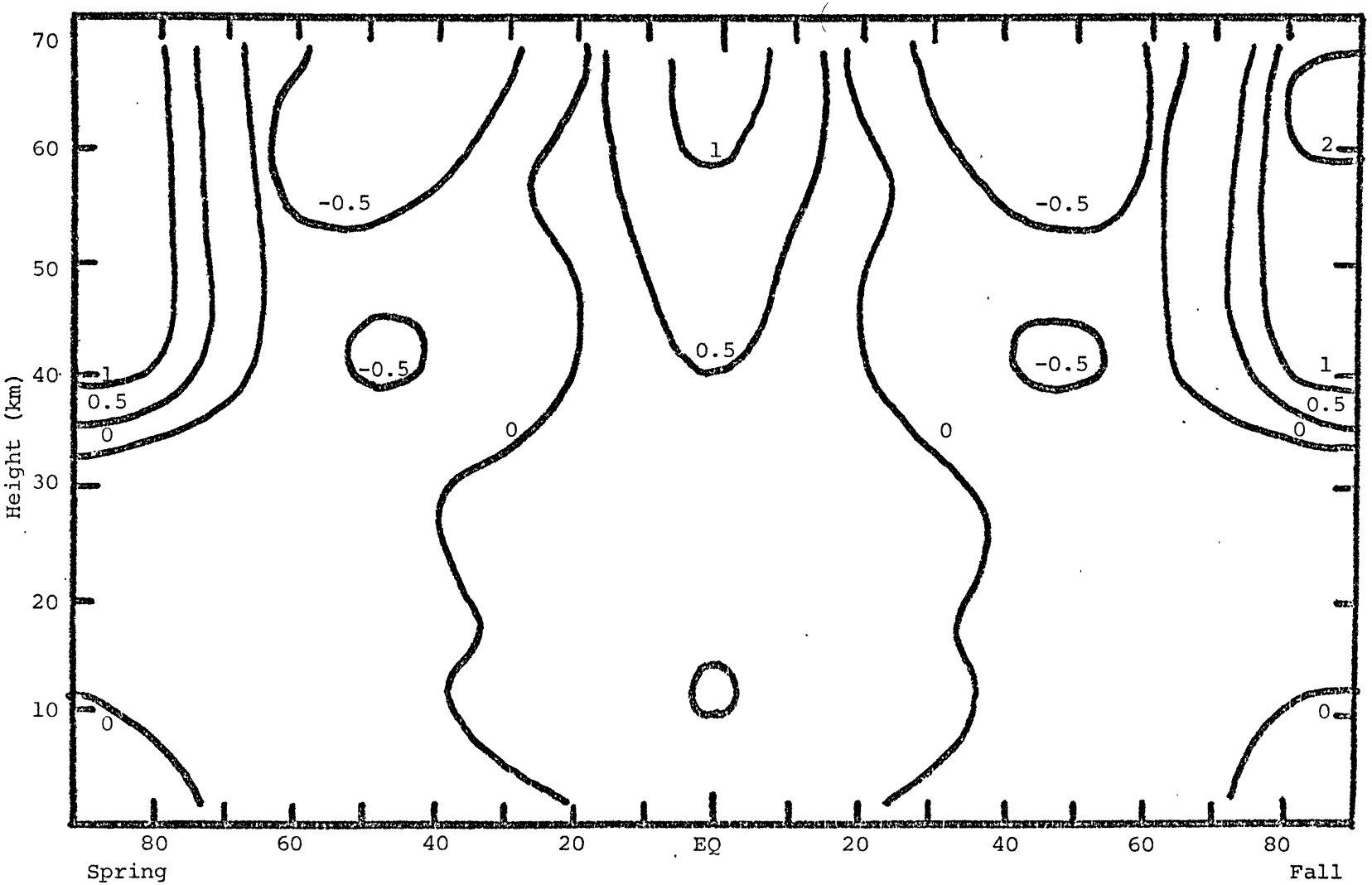

Figure 5: Lagrangian mean vertical wind velocities in cm/sed for spring and fall.

deserts may also act as sinks for atmospheric pollutants. Other chemical reactions, primarily in the stratosphere, destroy some of our tracers. The reaction with $O(^1D)$ was found by Golombek (1982) to be less than 2% of the photodissociation destruction for $CFCl_3$ and less than 12% for CF_2Cl_2. It is very small for CCl_4.

We ensure that numerical errors are not occurring in our integration of the tracer continuity equation by printing out, at the beginning and end of each season, the total amount of tracer in the model atmosphere, the mass input due to anthropogenic sources, and the mass loss due to photochemical dissociation. Input minus loss always exactly balanced tracer increase.

III. Model Results

1. Model diagnostics

Our model was tested by running it for three consecutive years for the man-made pollutants carbon tetrachloride (CCl_4), trichlorofluoromethane ($CFCl_3$), and dichlorodifluoromethane (CF_2Cl_2). The model was evaluated by comparing the results to the data taken by the Atmospheric Lifetime Experiment (ALE). (Cunnold, et al, 1982a,b; Simmonds, et al, 1982)

The photodissociation lifetime was computed every 30 days of the model runs. The instantaneous photodissociation lifetime τ is defined as the total atmospheric content of tracer divided by the rate of photochemical destruction. Our computed lifetime values are 30 day averages. Annual averages were also calculated and are compared with previous estimates of the photodissociation lifetime. Unfortunately, atmospheric measurements still leave large uncertainties in our knowledge of the photodissociation lifetimes of these substances.

The trend, or percentage rate of increase, of a tracer is our most valuable diagnostic parameter because we can compare it with the trends being measured at the five global monitoring stations in the ALE network. The trend over a particular time period is defined as

$$(1/X)(dX/dt)=A$$

where A is a constant. It can be calculated by fitting our modeled concentrations to a line of the form

$$\ln X = At + B.$$

We have used a least squares curve fit to the mixing ratios at the end of each season for our three years of calculated data. We calculate a global trend based on the total atmospheric tracer content, surface trends corresponding to each of the five ALE sites, and a surface global trend. The surface global trend is an area weighted average of the ALE site surface trends. The same area-weighting is applied to the ALE observations for

comparison.

2. ALE Data

The ALE network was set up to provide accurate measurements of atmospheric halocarbons over a time period long enough to determine their trends and lifetimes. Measurements of trichlorofluoromethane, dichlorodifluoromethane, carbon tetrachloride, nitrous oxide, and methyl chloroform are taken three to four times a day using elctron-capture gas chromatography. Concentrations are determined by comparison with an on-site standard. (Prinn et al, 1982)

The five operating stations are Adrigole, Ireland at a latitude of 52°N, Cape Meares, Oregon at 45°N, Ragged Point, Barbados at 13°N, the NOAA site in Americal Samoa at 14°S, and Cape Grim, Tasmania at 41°S. All sites except Oregon have been operating since July 1978 and three years of data have been obtained for them. Cape Meares, Oregon began operating in January 1980. Nineteen months of data have been obtained for this station. See Table 1 for the ALE station numbering system which will be used in the remainder of this thesis.

The trends fitted to the ALE station data are optimal estimations of a linear trend with a curvature term and an annual cycle. The data for Adrigole and Cape Meares have been combined to produce a composite single trend.

3. Initialization

Our model was initialized using the same initial two-dimensional concentration profiles as were used by Golombek (1982). Measured concentrations at four of the ALE stations for July 1978 were used as the initial horizontal profile by linearly interpolating between stations. Vertical profiles were from a one-dimensional model by Crutzen et al (1978) for our three pollutants. A second profile obtained from measurements by Fabian (1981) and Fabian et al (1981) at a location in Germany (~44°N) was also used for

Table 1: ALE station numbers and locations.

Station Number	Station Name	Location	Date at which measurements began
1	Adrigole, Ireland	52°N, 10°W	July, 1978
2	Cape Meares, Oregon	45°N,124°W	January,1980
3	Ragged Point, Barbados	13°N, 59°W	July, 1978
4	NOAA Site, American Samoa	14°S,171°W	July,1978
5	Cape Grim, Tasmania	41°S,145°E	July, 1978

the two chlorofluorocarbons. Two-dimensional initial profiles were obtained by multiplying the vertical profile by the ratio of the horizontal profile surface concentration to the vertical profile surface concentration for each model latitude. Initial horizontal and vertical profiles are shown in Tables 2 and 3.

4. Anthropogenic source

Anthropogenic release rates are based on reports of the Chemical Manufacturers Association and are summarized by Simmonds et al (1982) for carbon tetrachloride, by Cunnold et al (1982a) for $CFCl_3$, and by Cunnold et al (1982b) for CF_2Cl_2. Annual atmospheric releases for the years 1978 to 1981 are shown in Table 4. Our values are updated to those given in the February 1982 CMA report and thus are slightly different from Golombek's.

Our anthropogenic source distribution follows Golombek (1982) but is integrated over longitude for application to our two-dimensional model. The latitudinal distribution of the anthropogenic source in percent of total input is shown in Table 5.

5. Photodissociation

Photochemical dissociation is the chemical breakdown of a compound in the presence of ultraviolet radiation. The main reactions undergone by the halocarbons studied in our model are:

$$CCl_4 + h\nu \xrightarrow{J_{CCl_4}} CCl_3 + Cl$$

$$CFCl_3 + h\nu \xrightarrow{J_{CFCl_3}} CFCl_2 + Cl$$

$$CF_2Cl_2 + h\nu \xrightarrow{J_{CF_2Cl_2}} CF_2Cl + Cl.$$

The J values, or photodissociation coefficients, determine the reaction rates. J values are computed for a given latitude, level, and season by the following numerical integration over wavelength:

$$J_k(\mu_o) = \Sigma\ \sigma_k(\lambda)\ F(\mu_o, \lambda)$$

where σ_k is the absorption cross-section of species k, F is the solar flux at wavelength λ and solar angle to the zenith of $\arccos(\mu_o)$. Solar flux is

Table 2: Horizontal concentration profiles used for model initialization. Concentrations at ALE stations are measured monthly average mixing ratios for July 1978. Other mixing ratios are interpolated.

Latitude	ALE Station	CCl4 (pptv)	CFCl3 (pptv)	CF2Cl2 (pptv)
80.5°N		119.0	166.9	273.7
69.0°N		119.0	166.9	273.7
57.5°N	1	119.0	166.9	273.7
46.0°N		117.9	165.1	272.5
34.5°N		116.8	163.3	271.4
23.0°N		115.8	161.6	270.2
11.5°N	3	114.7	159.8	269.0
0.0		112.3	152.4	255.4
11.5°S	4	109.9	145.0	241.7
23.0°S		111.2	144.0	241.8
34.5°S		112.5	143.1	241.8
46.0°S	5	113.8	142.1	241.9
57.5°S		113.8	142.1	241.9
69.0°S		113.8	142.1	241.9
80.5°S		113.8	142.1	241.9

Table 3: Vertical concentration profiles used for model initialization. (from Crutzen et al, 1978 or Fabian, 1981 and Fabian et al, 1981)

level	height (km)	CCl_4 CRU (pptv)	$CFCl_3$ FAB (pptv)	$CFCl_3$ CRU (pptv)	CF_2Cl_2 FAB (pptv)	CF_2Cl_2 CRU (pptv)
9	48.7					0.1
10	45.8				0.1	1.3
11	43.0				1.0	4.4
12	40.1	0.1			3.1	12.0
13	37.2	0.4		0.2	8.5	27.8
14	34.4	1.2	0.3	1.0	18.7	52.2
15	31.5	4.5	1.4	4.3	36.1	84.0
16	28.6	17.0	5.7	16.9	54.9	106.6
17	25.8	37.0	18.0	42.1	70.6	135.0
18	22.9	67.7	40.8	75.4	103.5	166.9
19	20.0	87.2	76.7	109.3	151.0	196.6
20	17.2	110.1	95.3	127.7	187.1	215.7
21	14.3	111.6	120.5	137.1	214.0	229.4
22	11.5	117.7	136.8	145.5	237.6	242.2
23	8.6	117.8	151.5	152.3	253.8	254.7
24	5.7	118.6	151.4	152.2	254.6	255.0
25	2.9	118.8	153.1	153.2	256.4	256.5
26	0.0	118.8	153.1	153.2	256.4	256.6

Table 4: Annual anthropogenic releases to atmosphere (10^9 gm/year).

year	CCl_4 (1)	$CFCl_3$ (2)	CF_2Cl_2 (3)
1978	99.2	294.6	384.9
1979	93.0	276.1	388.4
1980	97.2	264.3	392.5
1981	97.2*	264.3	412.2

References:

(1) Simmonds, et al (1982)
(2) Cunnold, et al (1982a)
(3) Cunnold, et al (1982b)

*-Estimated value.

Table 5: Latitudinal distribution of anthropogenic release in per cent for years 1978-1981. (from Golombek, 1982)

latitude	CCl_4	$CFCl_3$	CF_2Cl_2
80.5°N	0	0	0
69.0°N	0	0	0
57.5°N	15.09	15.09	15.24
46.0°N	41.25	41.25	41.58
34.5°N	21.13	21.13	21.26
23.0°N	7.11	7.11	6.08
11.5°N	8.89	8.89	7.60
0	1.19	1.19	1.50
11.5°S	1.19	1.19	1.50
23.0°S	1.19	1.19	1.50
34.5°S	2.11	2.11	2.60
46.0°S	0.85	0.85	1.10
57.5°S	0	0	0
69.0°S	0	0	0
80.5°S	0	0	0

computed as in Pitari and Visconti (1979) and includes the effects of Rayleigh scattering. Scattering by air molecules results in an increase in the apparent reflectivity of the lower atmosphere and surface of the earth. See Appendix B for a description of the solar flux calculation.

Seasonally averaged J values are obtained for each latitude by averaging instantaneous J values calculated for ten different zenith angles equally spaced for the daylight hours of the mid-season day. The mid-season day has a maximum solar zenith angle which is the average of the daily maximum solar zenith angles for that season.

The cross-sections for CCl_4 come from WMO (1981) and for $CFCl_3$ and CF_2Cl_2 from NASA (1979). The horizontal averages of our calculated J values for the Northern Hemisphere winter season are shown in Table 6.

6. Results for carbon tetrachloride

The photodissociation lifetime trend given by our model for carbon tetrachloride is shown in Figure 6. The lifetime is increasing slowly during the first 12 month of model integration as excess tracer introduced by the initialization is destroyed in the stratosphere. There is an obvious annual cycle in the lifetime trend. More photodissociation occurs in spring and fall than in summer and winter because stratospheric CCl_4 concentrations are considerably larger in the tropics than over mid-latitudes. When solar radiation strikes the tropics most directly, greater photodissociation occurs and the photochemical lifetime is smaller.

The annual average lifetime of CCl_4 given by our model is about 47.5 years. The best estimate of the lifetime of CCl_4 is 56 years based on the ALE data and a 9-box model by Simmonds, et al (1982). Golombek (1982) estimated 50 years.

The measured trends of CCl_4 t the five ALE stations are shown in Table 7 along with those predicted by our model. Our predicted trends are very close to the experimentally determined trends, though we are overpredicting

Table 6: Photochemical dissociation rates, J (sec^{-1}), and photochemical lifetimes, τ, horizontally averaged for December, January, and February as a function of height.

level	height (km)	J_{CCl_4}	τ_{CCl_4}	J_{CFCl_3}	τ_{CFCl_3}	$J_{CF_2Cl_2}$	$\tau_{CF_2Cl_2}$
1	71.6	9.5×10^{-6}	29 hr	2.6×10^{-6}	4.5 da	5.6×10^{-7}	21 da
2	68.7	9.1×10^{-6}	31 hr	2.6×10^{-6}	4.5 da	5.4×10^{-7}	21 da
3	65.9	8.8×10^{-6}	32 hr	2.8×10^{-6}	4.1 da	5.2×10^{-7}	22 da
4	63.0	8.6×10^{-6}	32 hr	2.8×10^{-6}	4.1 da	4.9×10^{-7}	24 da
5	60.1	8.2×10^{-6}	34 hr	2.8×10^{-6}	4.1 da	4.5×10^{-7}	26 da
6	57.3	8.0×10^{-6}	35 hr	2.8×10^{-6}	4.1 da	4.2×10^{-7}	28 da
7	54.4	7.7×10^{-6}	35 hr	2.7×10^{-6}	4.3 da	3.8×10^{-7}	30 da
8	51.6	7.1×10^{-6}	39 hr	2.5×10^{-6}	4.6 da	3.3×10^{-7}	35 da
9	48.7	6.1×10^{-6}	44 hr	2.3×10^{-6}	5.0 da	2.8×10^{-7}	41 da
10	45.8	5.6×10^{-6}	50 hr	2.1×10^{-6}	5.5 da	2.3×10^{-7}	50 da
11	43.0	4.9×10^{-6}	57 hr	1.8×10^{-6}	6.4 da	1.9×10^{-7}	61 da
12	40.1	3.6×10^{-6}	77 hr	1.4×10^{-6}	8.3 da	1.3×10^{-7}	89 da
13	37.2	2.6×10^{-6}	4.5 da	9.8×10^{-7}	12 da	8.9×10^{-8}	135 da
14	34.4	1.5×10^{-6}	7.7 da	6.1×10^{-7}	19 da	4.9×10^{-8}	236 da
15	31.5	8.2×10^{-7}	14 da	3.4×10^{-7}	34 da	2.5×10^{-8}	463 da
16	28.6	3.5×10^{-7}	33 da	1.7×10^{-7}	68 da	1.0×10^{-8}	3.2 yr
17	25.8	1.1×10^{-7}	105 da	4.6×10^{-8}	252 da	2.9x10-9	11 yr
18	22.9	2.5×10^{-8}	463 da	1.0×10^{-8}	3.2 da	6.1x10-9	52 yr
19	20.0	4.2×10^{-9}	7.5 yr	1.7×10^{-9}	19 yr	9.1×10^{-11}	348 yr
20	17.2	4.4×10^{-9}	72 yr	1.7×10^{-10}	187 yr	7.6×10^{-12}	4×10^{3} yr
21	14.3	2.0×10^{-10}	2×10^{3} yr	6.4×10^{-12}	5×10^{3} yr	2.8×10^{-13}	1×10^{5} yr
22	11.5	2.3×10^{-13}	1×10^{5} yr	6.9×10^{-14}	5×10^{5} yr	2.8×10^{-15}	1×10^{7} yr
23	8.6	6.0×10^{-16}	5×10^{7} yr	1.6×10^{-16}	2×10^{8} yr	6.2×10^{-18}	5×10^{9} yr
24	5.7	4.6×10^{-19}	7×10^{10}yr	1.0×10^{-19}	3×10^{11}yr	3.9×10^{-21}	8×10^{12}yr
25	2.9	4.5×10^{-23}	7×10^{14}yr	8.1×10^{-24}	4×10^{15}yr	3.1×10^{-25}	1×10^{17}yr
26	0	1.7×10^{-26}	2×10^{18}yr	1.7×10^{-27}	2×10^{19}yr	1.4×10^{-28}	2×10^{20}yr

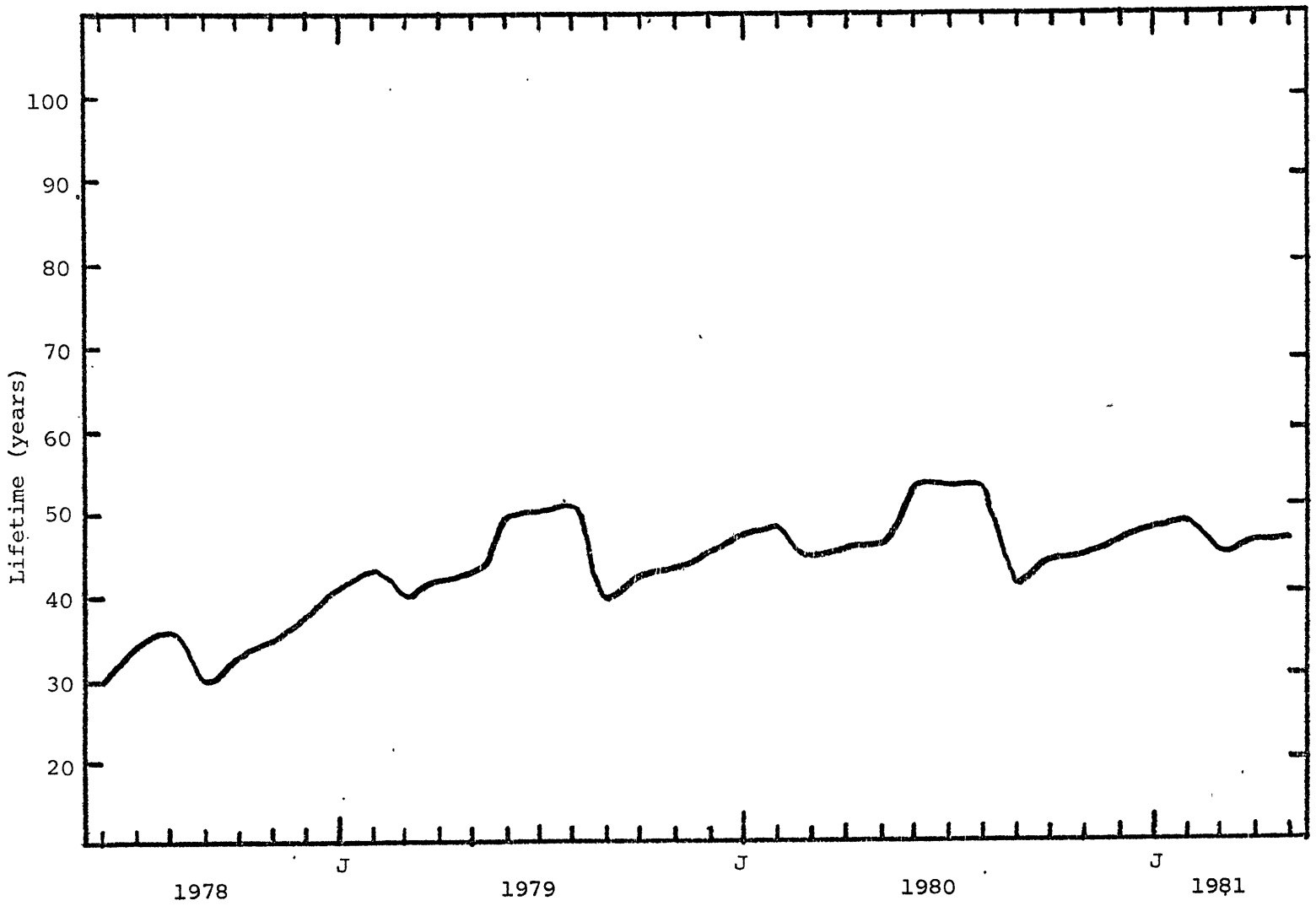

Figure 6: CCl_4 lifetime trends calculated by the model for June 1978 to May 1981.

Table 7: CCl_4 experimental and calculated trends in %/year, based on three years of data. Mixing ratios for May 1981 (m_{81}) are given in pptv.

ALE	Experimental		Calculated	
Station	Trend	m_{81}	Trend	m_{81}
1	2.03	132.3	2.07	132.6
2	2.03	125.0	1.82	132.3
3	2.10	122.7	2.19	127.8
4	1.83	117.4	2.01	120.7
5	1.22	116.5	1.31	116.2
Surface	1.78		1.82	
Global			0.93	

slightly at Station 4, American Samoa. The area-wieghted surface average trend is predicted to be 1.82% per year. The same average of the ALE site experimental trends is 1.78% per year. The calculated global trend for the integrated CCl_4 mass of the entire model atmosphere is 0.93% per year.

Figure 7 shows the two-dimensional field of CCl_4 mixing ratios at the end of May 1981 after three years of model integration. Mixing ratios at the ALE stations as measured and as predicted by the model for May 1981 are shown in Table 7 along with the trends. It can be seen that stratospheric concentrations of CCl_4 peak in the tropics, presumably due to strong upward transport by the Lagrangian mean circulation in this region. Ground level concentrations peak in the Northern Hemisphere because the largest portion of the anthropogenic release occurs there.

The contributions of the horizontal advection, horizontal diffusion, and vertical advection terms to tracer transport in the model have been evaluated for the end of May 1981. The flux due to advection crossing the equator is 4.27×10^{26} molecules per second compared with 1.62×10^{25} molecules per second due to diffusion. The total horizontal advective transport is 4.88×10^{27} molecules per second. The total horizontal diffusive transport is 2.52×10^{26} molecules per second. Total vertical transport, all due to advection, is 1.80×10^{27} molecules per second.

7. Results for trichlorofluoromethane

The lifetime trends for trichlorofluoromethane are shown in Figure 8. With the Fabian initial profile, our model stratosphere had too little tracer mass initially and therefore the lifetime was initially large and gradually decreased until the stratospheric mass deficit had been filled in by transport from lower levels. The trends for the two different initial profiles are converging slowly. After three years of model integration, they differ only by one year in the predicted lifetime values. An annual trend similar to that seen for CCl_4 is also evident for $CFCl_3$.

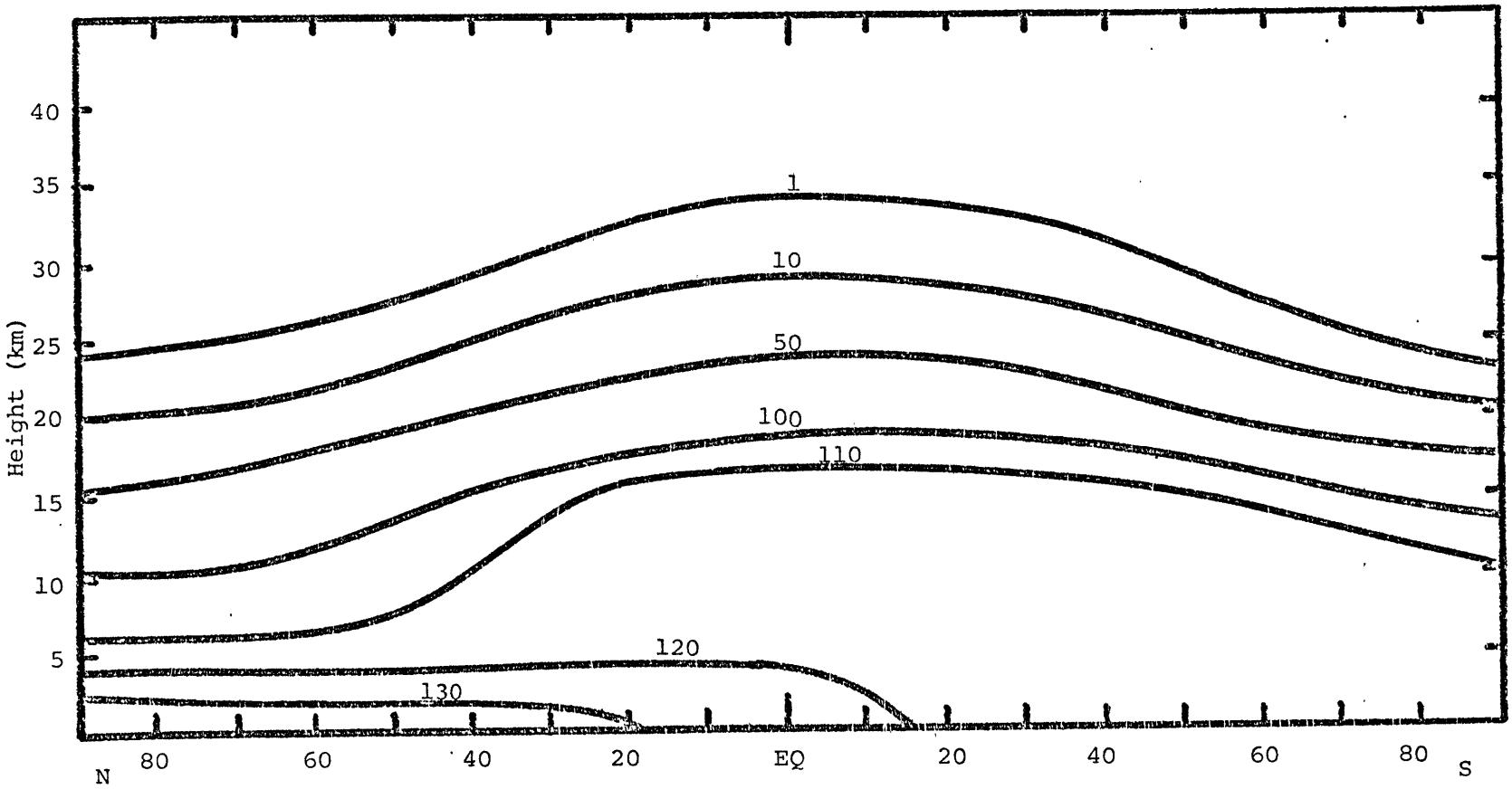

Figure 7: Calculated CCl_4 mixing ratios for May 1981 in pptv.

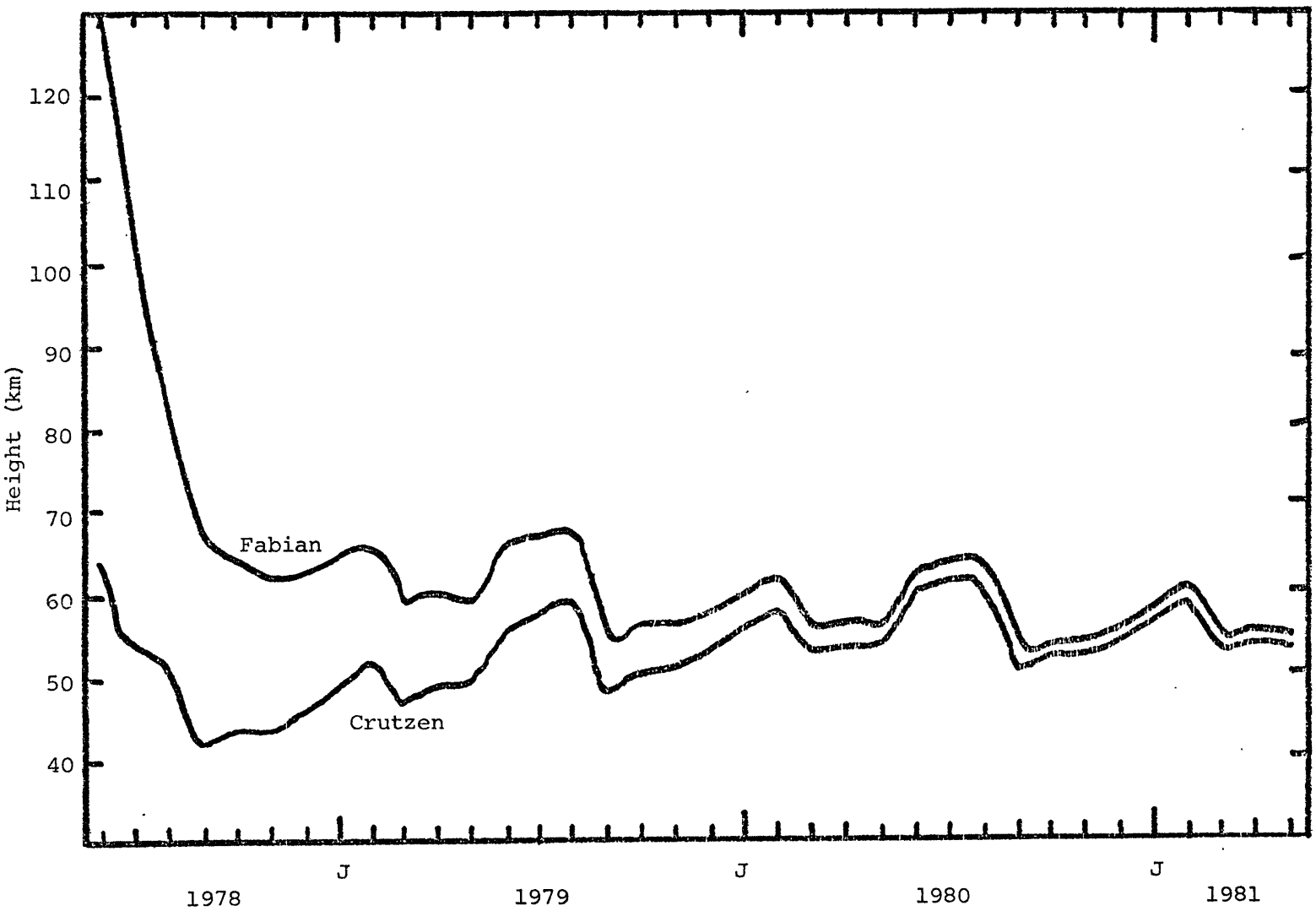

Figure 8: $CFCl_3$ lifetime trends calculated by the model using the Fabian and Crutzen initial profiles for June 1978 to May 1981.

The annual average lifetime for $CFCl_3$ estimated by our model is about 58 years. Golombek(1982) estimated the lifetime to be 78 years. Cunnold et al (1982) derived lifetime estimates based on the ALE data of between 66 and 71 years, with an uncertainty range of from 45 years to 145 years.

Experimental and calculated trends for $CFCl_3$ are shown in Table 8. The results with the Crutzen initial profile most closely match the experimental trends, though the trend at Station 4 is again overpredicted and that at Station 5 underpredicted. The predicted average surface trend is 5.25% per year with the Fabian initial profile and 5.88% per year with the Crutzen initial profile. The experimental surface trend is 5.83% per year and has been bracketed by our predicted surface trends. Predicted global trends are 5.51% per year with the Fabian initial profile and 5.15% per year with the Crutzen initial profile.

The two-dimensional field of $CFCl_3$ mixing ratios calculated for May 1981 for the Crutzen initial profile is shown in Figure 9. Surface mixing ratios at the ALE stations for May 1981 are shown in Table 8. Stratospheric concentrations also peak in the tropics for $CFCl_3$.

For May 1981, the predicted horizontal flux crossing the equator due to advection is 1.44×10^{26} molecules per second for the integration with the Crutzen initial profile. The flux crossing the equator due to diffusion is 2.31×10^{25} molecules per second. The total advective horizontal transport is 2.60×10^{27} molecules per second and the total diffusive horizontal transport is 2.54×10^{26} molecules per second. The total vertical transport is 2.70×10^{27} molecules per second.

8. Results for dichlorodifluoromethane

The calculated lifetime trends for dichlorodifluoromethane are shown in Figure 10. The lifetime trends for both initial profiles indicate an initial deficit of tracer mass in the model stratosphere, since both trends are initially dropping rapidly. The annual cycle in the lifetime trend of

Table 8: $CFCl_3$ experimental and calculated trends in %/year, based on three years of data. Mixing ratios for May 1981 (m_{81}) are given in pptv.

ALE	Experimental		Calculated-FAB		Calculated-CRU	
Station	Trend	m_{81}	Trend	m_{81}	Trend	m_{81}
1	4.98	192.1	4.61	213.0	5.21	216.8
2	4.98	188.7	4.11	212.6	4.72	216.4
3	5.65	183.8	4.96	198.5	5.66	202.3
4	6.05	175.0	5.84	179.0	6.50	182.9
5	6.80	173.0	5.81	167.7	6.40	171.5
Surface	5.83		5.25		5.88	
Global			5.51		5.15	

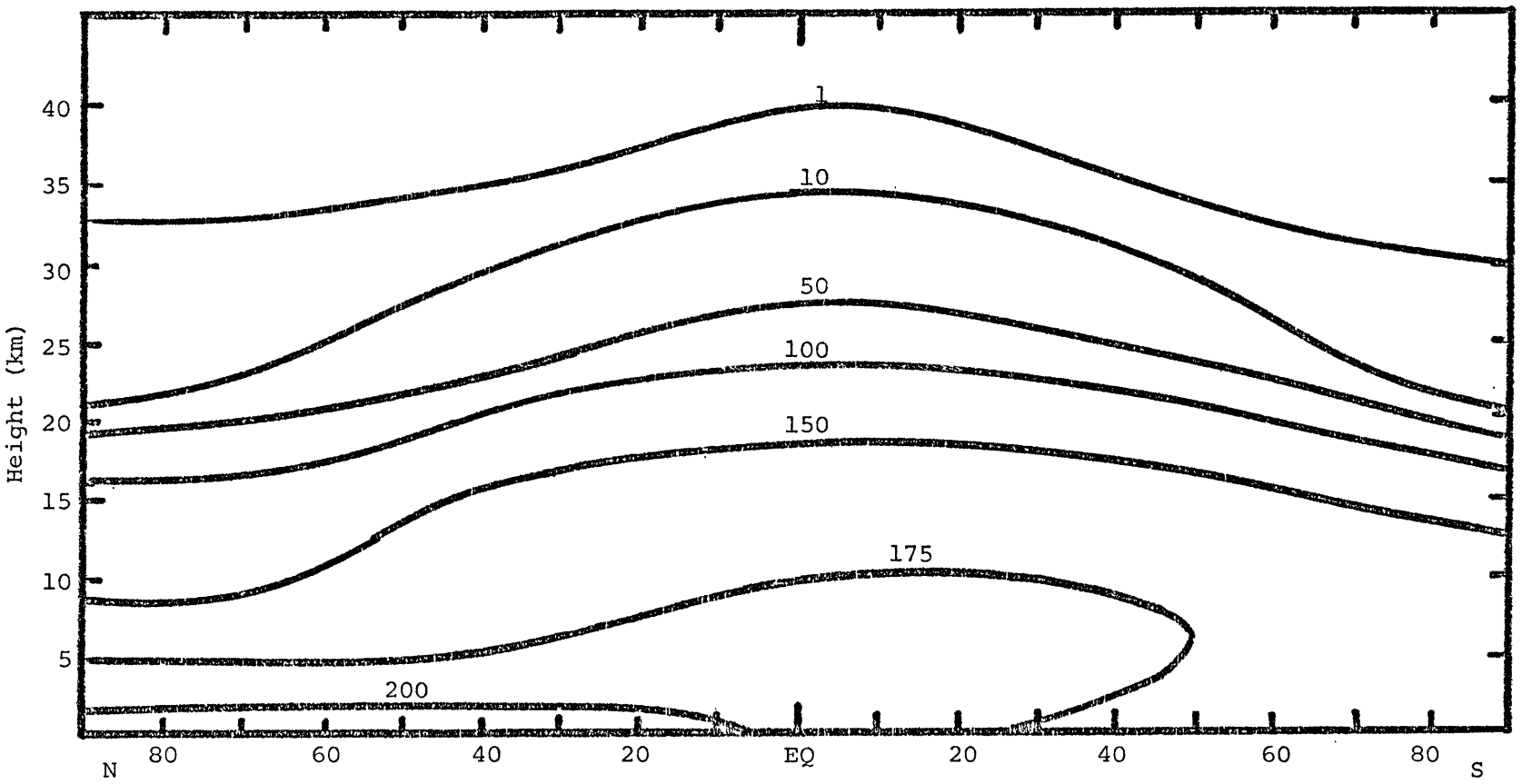

Figure 9: Calculated $CFCl_3$ mixing ratios in pptv for May 1981 using the Crutzen initial profile.

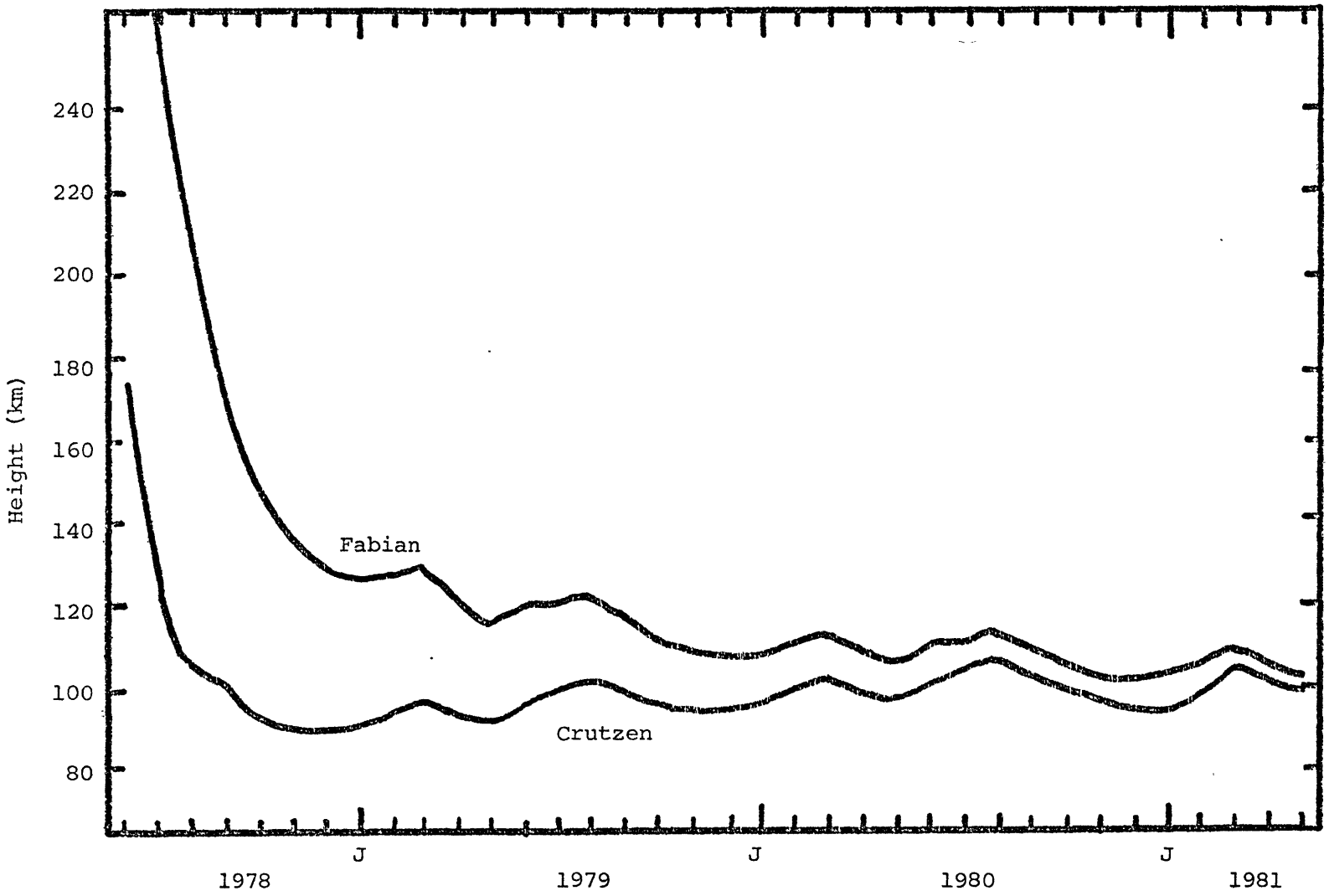

Figure 10: CF_2Cl_2 lifetime trends calculated by the model using the Fabian and Crutzen initial profiles for June 1978 to May 1981.

CF_2Cl_2 is much less distinct than for CCl_4 or $CFCl_3$ because stratospheric concentrations do not peak as strongly in the tropics for CF_2Cl_2.

The lifetime trends for the two initial profiles converge to an annual average of 104 years. Golombek (1982) found a lifetime of about 220 years for CF_2Cl_2. Cunnold et al (1982b) estimated a lifetime of 1430 years by the trend technique and 67 years by the inventory technique, with uncertainties ranging from a value of 51 years to infinity.

Table 9 shows experimental and calculated trends for CF_2Cl_2. Here our predicted trends with the Fabian initial profile are quite close to the experimental trends for all stations except Station 3, Barbados, where we are overpridicting. Results for the Crutzen initial profile show trends that are too large for all ALE stations. Predicted surface trends are 6.14% per year for the Fabian initial profile and 6.61% per year for the Crutzen initial profile. The experimental surface trend is 6.00% per year. Predicted global tracer content trends are 6.03% per year and 5.76% per year for the Fabian and Crutzen initial profiles, respectively.

Figure 11 shows the two-dimensional concentration field for May 1981 for the Fabian initial profile. Because CF_2Cl_2 has much smaller photodissociation coefficients than $CFCl_3$ or CCl_4, we find concentrations of up to 11 pptv at the top boundary of the model.

The horizontal tracer fluxes crossing the equator ,as predicted for May 1981, using the Fabian initial profile, are 2.43×10^{26} molecules per second due to advection and 3.78×10^{25} molecules per second due to diffusion. The total horizontal advective transport is 4.43×10^{27} molecules per second and the total diffusive transport is 3.81×10^{26} molecules per second. The total vertical transport is 4.66×10^{27} molecules per second.

Table 9: CF_2Cl_2 experimental and calculated trends in %/year, based on three years of data. Mixing ratios for May 1981 (m_{81}) are given in pptv.

ALE	Experimental		Calculated-FAB		Calculated-CRU	
Station	Trend	m_{81}	Trend	m_{81}	Trend	m_{81}
1	5.89	324.1	6.07	362.9	6.54	367.3
2	5.89	318.4	5.61	362.3	6.09	366.7
3	5.52	318.4	5.61	362.3	6.09	341.5
4	6.32	296.2	6.44	304.6	6.94	309.0
5	6.24	292.9	6.18	285.9	6.56	290.5
Surface	6.00		6.14		6.61	
Global			6.03		5.76	

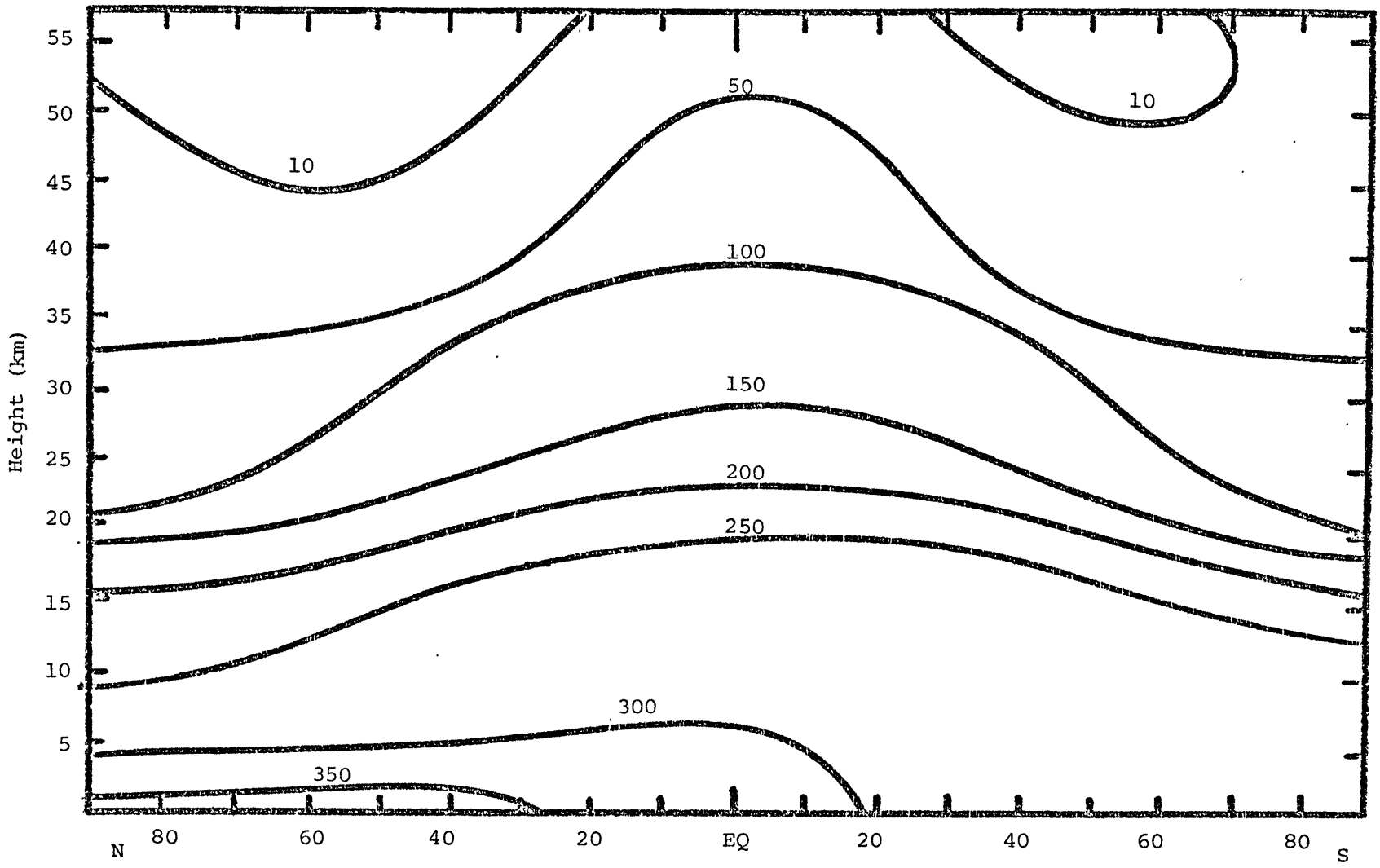

Figure 11: Calculated CF_2Cl_2 mixing ratios in pptv for May 1981 using the Fabian initial profile.

IV. Summary and Conclusions

Our model has done a good job of predicting global trends for the pollutants carbon tetrachloride, trichlorofluoromethane, and dichlorodifluoromethane. Our results compare favorably with those obtained by Golombek (1982) from a three-dimensional model. In fact, our predicted trends for CCl_4 are closer to the measured trends than are Golombek's. Also, he consistently overpredicted the trends at Station 5, Tasmania, where we have sometimes predicted well and sometimes underpredicted slightly.

We have shown that an advective model using Lagrangian mean winds can be used for studying the global transport of atmospheric pollutants. A Lagrangian model eliminates the need to know both a set of mean winds and a set of diffusion coefficients. Diffusion coefficients are not known with any certainty. Unfortunately, Lagrangian winds are not known accurately either. However, the success of our two-dimensional model gives credibility to the Lagrangian mean wind velocities that we have used.

Appendix A: Calculation of Lagrangian Velocities

Lagrangian mean velocities may be calculated from diabatic heating rates, as was done by Olaguer, starting with the thermodynamic equation and the continuity equation.

$$\frac{\partial \bar{\theta}^L}{\partial t} + \bar{v}^L \frac{\partial \bar{\theta}^L}{\partial y} + \bar{w}^L \frac{\partial \bar{\theta}^L}{\partial z} = \bar{Q}^L$$

$$\frac{1}{\cos\phi} \frac{\partial}{\partial y}(\bar{v}^L \cos\phi) + \frac{1}{\rho_o} \frac{\partial}{\partial z}(\rho_o \bar{w}^L) = 0$$

where $\bar{\theta}^L$=the Lagrangian mean potential temperature,

$\bar{Q}^L$=the Lagrangian mean diabatic heating rate,

$\bar{v}^L$=the Lagrangian mean meridional velocity,

$\bar{w}^L$=the Lagrangian mean vertical velocity,

ϕ =latitude,

ρ_o=density of the basic state.

The relationship between the Lagrangian mean and the zonal mean for either θ or Q can be written as:

$$\bar{A}^L \sim \bar{A} + \frac{\partial}{\partial y}\left(\frac{\overline{\Psi' A'}}{\bar{u}}\right) = \bar{A} + \bar{A}^S$$

where the overbar denotes a zonal mean and a prime denotes the deviation from the zonal mean. Ψ' is the perturbation stream function and $\bar{u}$ is the mean zonal wind velocity. $\bar{A}^S$ is known as the Stoke's correction.

By introducing a Lagrangian stream function $\bar{\Psi}^L$ such that

$$\rho_o \bar{v}^L \cos\phi = -\partial \bar{\Psi}^L / \partial z$$

$$\rho_o \bar{w}^L \cos\phi = \partial \bar{\Psi}^L / \partial y,$$

equation (1) may be rewritten as

$$\rho \cos\phi \frac{\partial \bar{\theta}^L}{\partial t} + \frac{\partial \bar{\theta}^L}{\partial z}\frac{\partial \bar{\Psi}^L}{\partial y} - \frac{\partial \bar{\theta}^L}{\partial y}\frac{\partial \bar{\Psi}^L}{\partial z} = \rho \bar{Q}^L \cos\phi.$$

This equation is evaluated numerically on a grid of 26 levels and 15 latitudes. The term $\partial \bar{\theta}^S / \partial y$ cannot be included in the calculations because it is a wave property with a vertical scale smaller than the resolution of

the model, therefore $\overline{\theta}^S$ will be neglected. If only solstice conditions are evaluated, $\partial\overline{\theta}/\partial t$ can be neglected, and equation (6) reduces to:

$$\frac{\partial\overline{\theta}}{\partial z}\frac{\partial\overline{\Psi}^L}{\partial y} - \frac{\partial\overline{\theta}}{\partial y}\frac{\partial\overline{\Psi}^L}{\partial z} = \rho_o\overline{Q}^L\cos\phi.$$

$\overline{Q}^L$ includes the effects both of thermal forcing and of wave dissipation.

Equation (7) was integrated separately for each hemisphere using the method of characteristics, subject to the boundary condition that $\overline{\Psi}^L$ vanish at all model boundaries.

Appendix B: Calculation of Solar Flux

Solar flux is computed using the method of Pitari and Visconti (1979) and includes the effects of Rayleigh scattering. Scattering by air molecules results in an increase in the apparent reflectivity of the earth. Upward and downward solar fluxes are therefore modified.

For each height z the atmosphere is divided into two layers: layer 1 from ∞ to z and layer 2 from z to the ground. For each layer i we define its total reflectivity $\bar{R}_i(\mu_o)$ and its reflectivity when illuminated from below R_i^*.

$$\bar{R}_i(\mu_o) = 2\int_0^1 R_i(\mu,\mu_o)\mu \, d\mu$$

$$R_i^* = 2\int_0^1 \bar{R}_i(\mu_o)\mu_o \, d\mu_o$$

R_c is the combined reflectivity of the ground and the atmosphere below height z.

$$R_c(\mu_o) = \bar{R}_2(\mu_o) + [1-\bar{R}_2(\mu_o)](1-R_2^*)A/(1-R_2^*A)$$

where A is the albedo of the earth's surface.

$\bar{R}_i(\mu_o)$ can be determined by a simple function

$$\bar{R}_i(\mu_o) = A(\tau_R)/[B(\tau_R)+\mu_o]$$

where A and B are given in Table 10 and τ_R is the Rayleigh optical thickness for each level. With this function for $\bar{R}_i(\mu_o)$, R_i^* can be found by integration to be

$$R_i^* = 2A(\tau_R)+2A(\tau_R)B(\tau_R)\ln\{B(\tau_R)/[1+B(\tau_R)]\}.$$

The transmission factors for direct radiation T_i and diffuse radiation T_i^* are

$$T_1 = \exp[-\tau_{dir}(\infty,z)/\mu_o]$$

$$T_i^* = \exp[-M_1\tau_{dir}(\infty,z)/\mu_o]$$

$$T_2 = \exp[-\tau_{dir}(z,0)/\mu_o]$$

$$T_2^* = \exp[-M_2\tau_{dir}(z,0)/\mu_o]$$

where $\tau_{dir}(\infty,z)=N_{O_3}(z)\sigma_{O_3}+N_{O_2}(z)\sigma_{O_2}$

$\tau_{dir}(z,0)=[N_{O_3}(0)-N_{O_3}(z)]\sigma_{O_3}+[N_{O_2}(0)-N_{O_2}(z)]\sigma_{O_2}$.

N_{O_3} and N_{O_2} are the columnar densities of O_3 and O_2 and σ_{O_3} and σ_{O_2} are the corresponding cross sections. M is the magnification factor for diffuse radiation and is a function of optical thickness. Average values of M for five optical thickness intervals are shown in Table 11, as based on the curve reported by Kondratiev (1969).

The reflectivity seen at height z is given by

$$R_z=T_2T_2^*R_c,$$

taking into account the absorption between z and the ground.

Upward and downward direct fluxes are given by

$$F_u = \mu_o F_o T_1 R_z M_2 (1-R_1)/(1-R_1^*R_z)$$

$$F_d = \mu_o F_o T_1 (1-R_1)/(1-R_1^*R_z).$$

The diffuse component of the downward flux is

$$F_d^{dif} = F_d/T_1 - \mu_o F_o \exp(-\tau_R/\mu_o).$$

The total downward flux is

$$F_d = \mu_o F_o T_1 \exp(-\tau_R/\mu_o) + F_d^{dif} T_1^* M_1$$

$$= \mu_o F_o (T_1-T_1^*M_1)\exp(-\tau_R/\mu_o) + \mu_o F_o T_1^* M_1 (1-R_1)/(1-R_1^*R_z).$$

The total flux is therefore

$$F = F_u + F_d$$

$$= \mu_o F_o (T_1-M_1T_1^*)\exp(-\tau_R/\mu_o) + \mu_o F_o (M_1T_1^*+M_2T_1R_z)(1-R_1)/(1-R_1^*R_z).$$

Table 10: Values of A and B as a function of Rayleigh optical thickness τ_R (from Pitari and Visconti, 1979)

τ_R	A	B	τ_R	A	B
0.0214	0.0106	0.0113	2.2	1.424	1.706
0.05	0.0251	0.026	2.4	1.578	1.879
0.1	0.0502	0.052	2.6	1.735	2.055
0.15	0.0757	0.080	2.8	1.894	2.232
0.2	0.101	0.110	3.0	2.053	2.405
0.4	0.203	0.239	3.5	2.459	2.849
0.6	0.316	0.382	4.0	2.883	3.309
0.8	0.436	0.535	5.0	3.737	4.225
1.0	0.562	0.693	7.0	5.4307	6.01
1.2	0.695	0.857	9.0	7.134	7.793
1.4	0.832	1.02	11.0	8.779	9.523
1.6	0.975	1.18	13.0	10.447	11.227
1.8	1.11	1.36	15.0	12.05	12.89
2.0	1.27	1.531	16.0	12.86	13.73

Table 11: Magnification factor M as a function of optical thickness interval τ_R (from Pitari and Visconti, 1979)

$\Delta\tau_R$	0-0.07	0.07-0.2	0.2-1.0	1.0-3.5	3.5-
M	2	1.8	1.5	1.35	1.2

References

Andrews, D.G. and M.E. McIntyre, 1976: Planetary waves in horizontal and vertical shear: The generalized Eliassen-Palm relation and the mean zonal acceleration. J. Atm. Sci., 33, 2031-2048.

Crutzen, P.J., I.S.A. Isaksen, and J.R. McAfee, 1978: The impact of the chlorocarbon industry on the ozone layer. J. Geophys. Res., 83, 345-363.

Cunnold, D.M., R.G. Prinn, R.A. Rasmussen, P.G. Simmonds, F.N. Alyea, C.A. Cardilino, A.J. Crawford, P.J. Fraser, and R.D. Rosen, 1982a: The Atmospheric Lifetime Experiment, IV: Lifetime methology and application ot three years of $CFCl_3$ data. Submitted to J. Geophys. Res.

Cunnold, D.M., R.G. Prinn, R.A. Rasmussen, P.G. Simmonds, F.N. Alyea, C.A. Cardelino, and A.J. Crawford, 1982b: The Atmospheric Lifetime Experiment, V: Results for CF_2Cl_2 based on three years data. Submitted to J. Geophys. Res.

Dopplick, 1972: Radiative heating of the global atmosphere. J. Atm. Sci., 29, 1278-1294.

Dunkerton, T., 1978: On the mean meridional mass motions of the stratosphere and mesosphere. J. Atm. Sci., 35, 2325-2333.

Dutsch, H., 1971: Photochemistry of atmospheric ozone. Adv. in Geophysics, 15, Academic Press, 219-322.

Fabian, P., 1981: Atmospheric sampling. Adv. Space Res., 1, 17-27.

Fabian, P., R. Borchers, G. Flentje, W.A. Matthews, W. Seiler, H. Geihl, K. Bunse, F. Muller, U. Schmidt, A. Volz, A. Khedim, and F.J. Johnen, 1981: The vertical distribution of stable gases at mid-latitudes. J. Geophys. Res., 86, 5179-5184.

Golombek, A., 1982: A global three-dimensional model of the circulation and chemistry of long-lived atmospheric species. PhD Thesis, MIT.

Holton, J.R., 1981: An advective model for two-dimensional transport of stratospheric trace species. J. Geophys. Res., 86, 11989-11994.

Kondratiev, K. Ya., 1969: Radiation in the Atmosphere. Academic Press, 912 pp.

Lorenz, E.N., 1971: An N-cycle time-differencing scheme for stepwise numerical integration. Mon. Wea. Rev., 99, 644-648.

Mahlman, J.D. and W.J. Moxim, 1978: Tracer simulaton using a global general circulation model: Results from a midlatitude instantaneous source experiment. J. Atm. Sci., 35, 1340-1378.

NASA, 1979: The Stratosphere: Present and Future. NASA Reference Publication 1049.

Olaguer, E.P., 1982: A Lagrangian mean description of stratospheric tracer transport. Master's Thesis, MIT.

Pitari, G. and G. Visconti, 1979: A simple method to account for Rayleigh scattering effects on photodissociation rates. J. Atm. Sci., 36, 1803-1811.

Pitari, G. and G. Visconti, 1980: A two-dimensional model of the distribution of trace gases in the stratosphere and troposphere. Il Nuovo Cimento, 3, 541-571.

Prinn, R.G., R.A. Rasmussen, R.D. Rosen, P.G. Simmonds, F.N. Alyea, C.A. Cardelino, A.J. Crawford, D.M. Cunnold, P.J. Fraser, and J. E. Lovelock, 1982: The Atmospheric Lifetime Experiment, I: Introduction and Overview. Submitted to J. Geophys. Res.

Simmonds, P.G., F.N. Alyea, C.A. Cardelino, A.J. Crawford, D.M. Cunnold, B.C. Lane, J.E. Lovelock, R.G. Prinn, and R.A. Rasmussen, 1982: The Atmospheric Lifetime Experiment, VII: Results for carbon tetrachloride based on three years data. Submitted to J. Geophys. Res.

Tung, K.K., 1982: On the two-dimensional transport of stratospheric trace gases in isentropic coordinates. J. Atm. Sci., 39, 2330-2355.

WMO, 1981: The Stratosphere 1981, Theory and Measurements. Report No. 11.